



OPEN

# Enzyme-catalysed mineralisation experiment study to solidify desert sands

Linchang Miao , Linyu Wu & Xiaohao Sun 

Sandstorms are meteorological phenomena common in arid and semi-arid regions and have been recognized severe natural disasters worldwide. The key problem is how to control and mitigate sandstorm natural disasters. This research aims to mitigate their development by improving surface stability and soil water retention properties through soil mineralization. The enzymatic induced carbonate precipitation (EICP) is proposed to solidify desert sands and form a hard crust layer on the surface of desert sands. In contrast to micro-induced carbonate precipitation commonly used at room temperatures, EICP had high production efficiency and productivity at a broader temperature range (10–70 °C ±) and significantly improves material water retention properties, which was more suitable to desert environment. Results demonstrate that the enzyme-catalysed mineralisation method can be better resistance to high winds as the number of spraying times increased.

Sandstorm is a severe worldwide natural disaster because of land degradation in arid, semi-arid areas. Globally degraded/desertified land area makes up  $6.1 \times 10^7$  km<sup>2</sup>, covering nearly 41% of Earth's land surface and affecting approximately 38% of the world's population<sup>1,2</sup>. Desertification endangers ecosystem function and influences economic development and stability in arid and semi-arid areas<sup>3–5</sup>. The sandstorm occurs when a front or other strong wind system blows loose sand and dirt from a dry surface<sup>6</sup>. In the north of China, sand and dust from East/Central Asia is frequently transported by sweeping sandstorms over long distances on the scale of thousands of kilometers<sup>7</sup>, even arriving to Japan and Korea across the sea, spreading into the Pacific Ocean, North America, Greenland, and the European Alps<sup>8</sup>. In May 2007, a strong sand and dust storm (SDS) event in Taklimakan Desert, the Xinjiang Uygur Autonomous Region of China, traveled more than in one full circuit around the globe in about 13 days<sup>9</sup>.

Controlling land degradation and mitigating sandstorm remain global challenges today<sup>5</sup>. According the different mechanisms of controlling land degradation, Grainger<sup>10</sup> summarized the three prevailing methods for combating desertification: engineering, vegetation, and chemical methods. Engineering methods cost a lot of human and material resources. Some researchers, such as Deléglise et al.<sup>11</sup>, Liu et al.<sup>12</sup>, Verdoodt et al.<sup>13</sup>, Witt et al.<sup>14</sup>, think that grazing enclosure is an effective, simple, and direct method to control desertification in grasslands and restore vegetation. However, some studies in grasslands have shown that not all plant communities exhibit the same classic vegetation change patterns and regional differences and the influence of vegetation and soil properties for grazing enclosures have to be studied<sup>12,15–17</sup>. In addition, engineering and vegetation methods cannot be moved and reset according to the surface form and condition of sand accumulation in the field, therefore the function of engineering and vegetation methods for controlling desert sand will be reduction and failure over time.

In recent decade, the microbially-induced calcite precipitation (MICP) method has emerged as an alternative method for improving soil properties<sup>18–24</sup>. MICP is a biogeochemical process which essentially promotes metal ions to bind with acid radical ions to form calcium carbonate minerals<sup>25,26</sup>. The hydrolysis of urea by introduced urease-producing bacteria (e.g., *Sporosarcina pasteurii* (*S. pasteurii*) and *Bacillus megaterium* (*B. megaterium*)) is one of the most popular methods to induce carbonate precipitation<sup>27</sup>. It is widely thought that carbonate precipitation has significant potential as an important method of biomineralization<sup>28,29</sup>. But MICP are very complex and time consuming processes that frequently require special temperature environments. However, EICP has high productivity of calcium carbonate minerals at broader temperatures (ranging from 10 to 70 °C), which was more suitable to desert environment<sup>30</sup>. EICP involves mixing the soil with urea, calcium chloride (CaCl<sub>2</sub>), and urease enzyme<sup>31–34</sup>.

Institute of Geotechnical Engineering, Southeast University, Nanjing, Jiangsu, China. ✉ email: Lc.miao@seu.edu.cn

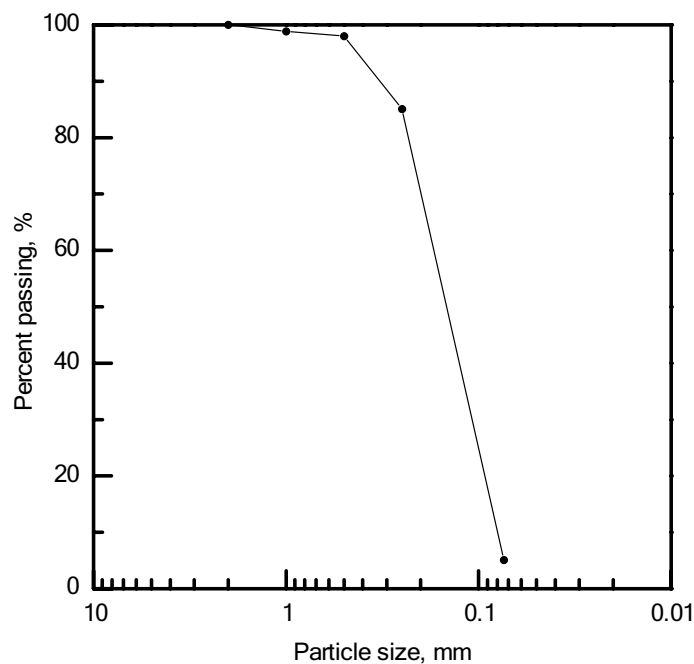


**Figure 1.** Particle size distribution of Ningxia desert sand.

Name	Specific gravity	Water content (%)	Stacking density ( $\text{kg m}^{-3}$ )	pH value
Desert sand	2.65	0.5%	1,440.3	8.39

**Table 1.** Physical and chemical properties of Desert sand of Ningxia. Specific gravity means the ratio of the mass of the soil particles dried at 105–110 °C to the mass of pure water at 4 °C.

Name	SiO <sub>2</sub>	Al <sub>2</sub> O <sub>3</sub>	CaO	Fe <sub>2</sub> O <sub>3</sub>	MgO	K <sub>2</sub> O	Na <sub>2</sub> O
%	69.8	12.5	2.67	2.98	2.16	2.78	1.17

**Table 2.** Mineral components of Desert sand of Ningxia.

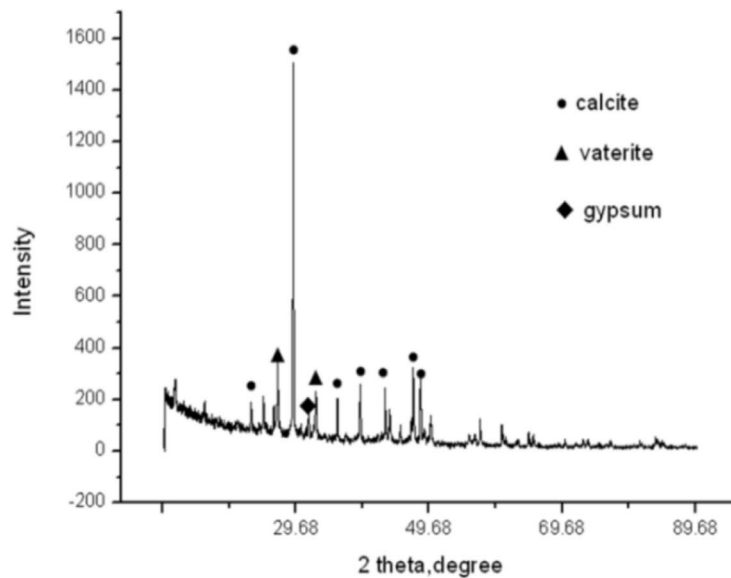
To improve the options for mitigating sandstorm disasters, this paper explored EICP for solidifying desert sands. Experiments to solidify desert sand were conducted in the laboratory with an enzyme solution followed by a urea–calcium acetate solution for different solidification models. The objective of EICP desert sand solidification is to form a hard crust layer on the sand surface to combat wind erosion. Curing effects on solidified desert sand by EICP were evaluated by wind tunnel testing, drying–wetting cycle testing, and water retention feature testing. The effectiveness of EICP, in particular on sand water retention, wind resistance, and environment stability were closely examined. Simultaneously, EICP desert sand solidification is an environmental friend method.

## Results

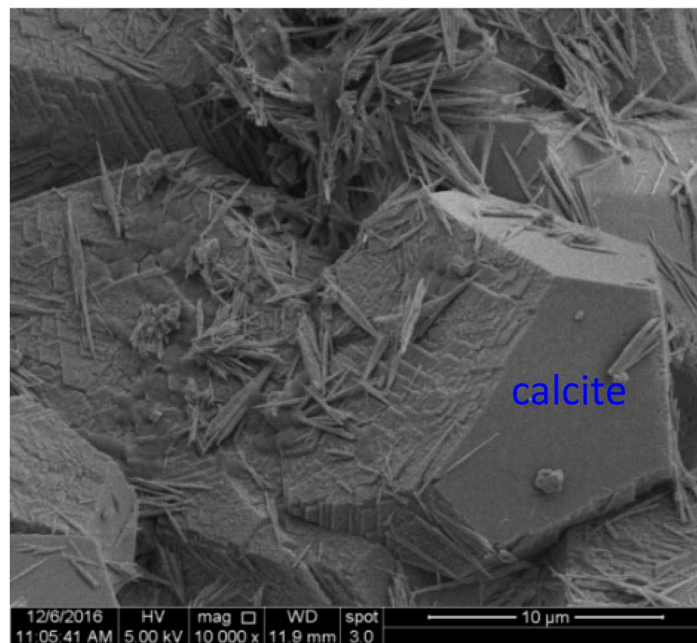
**Experimental materials.** Tests reported in this paper were performed on desert sand collected from the Tengger Desert in China's Ningxia Hui Autonomous Region, which is the fourth largest desert in China. Desert sand is fine sand whose particle size distribution is shown in Fig. 1. The physical and chemical properties of Tengger Desert desert sand are listed in the Table 1. Table 2 refers to its mineral components.

**Soil mineralization of EICP.** X-ray diffraction (XRD) pattern and scanning electron microscope (SEM) analysis confirmed that the calcite precipitation was deposited in the desert sand samples by EICP solidification (Fig. 2). SEM showed that the calcite was deposited between desert sand particles and increased their bonding forces. Calcite was sprayed in 6 g, 14 g, and 25 g increments two, four, and six times for the EICP mixture solution, respectively, and the volume increased as spraying times increased.

**Water retention capacity of EICP solidified desert sands.** In deserts, the water retention capacity of natural desert sand is very low and it is easily removed by the wind. The EICP mineralisation method was able



(a) X-ray diffraction (XRD) pattern analysis.



(b) SEM photo.

**Figure 2.** X-ray diffraction (XRD) pattern analysis and scanning electron microscope (SEM) solidification desert sand of EICP.

to solve the blown sand problem. Figure 3 shows the soil–water retention curve (SWRC) for EICP solidified desert sand. The residual volumetric water content was 6.1% for solidified desert sand and only 2.0% for natural desert sand. The improved water retention capacity of solidified desert sand was confirmed by SEM in Fig. 2. The calcite crystals induced by EICP filled gaps between sand particles and altered the pore structure of natural desert sand. Pores may have been connected, causing water and pore-water to easily evaporate and lose most moisture at the site. The solidified desert sand formed an aggregate of desert sand bonded by calcite crystals, however, and pore structure was different from the natural desert sand. The partial pores solidified desert sand may have been closed or semi-closed. Therefore, the solidified desert sand had improved water retention capacity. Improvements using EICP could facilitate the planting of vegetation to improve the environment in arid and semi-arid areas.

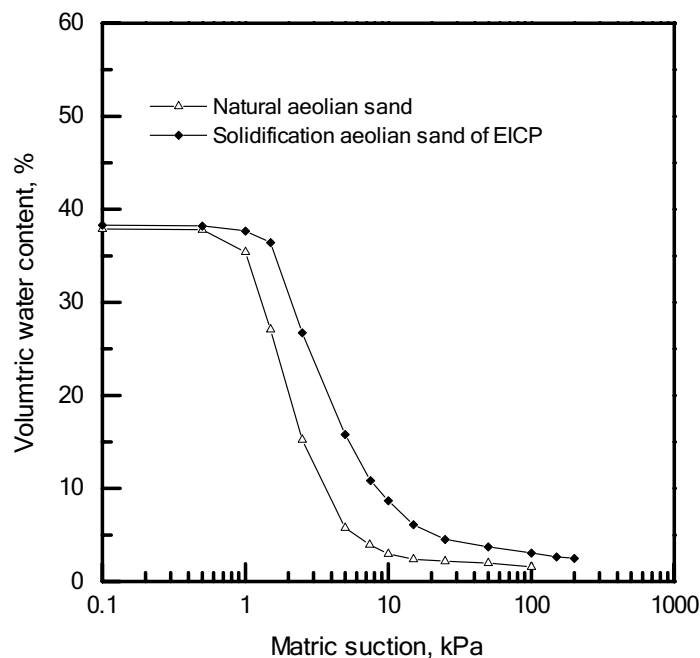


**Figure 3.** Soil–water retention curves of natural and EICP solidified desert sand.

Spraying times of EICP solution	Initial mass of desert sand (g)	Mass of after spraying (g)	Increment of calcium carbonate (g)
0	2,730	2,730	0
2	2,730	2,736	6
4	2,730	2,744	14
6	2,730	2,755	25

**Table 3.** The mass variations of solidification desert sand samples of EICP.

**Effects of EICP solidified desert sands.** This study tested solidified desert sand using EICP mineralization technology. The objective was to identify an effective and environmentally responsible technology to control sandstorm disasters. Results demonstrated that the enzyme-catalysed mineralisation method could be used for sandstorm impact reduction and improved water retention capacity in arid and semi-arid areas. (1) EICP soil mineralization can improve the surface stability of desert sand. The calcite added by EICP deposits between particles of desert sand formed an aggregate that alters the sand structure. (2) The soil–water retention curves for solidified desert sand showed that the EICP method enhanced water retention capacity. (3) EICP soil mineralization can be used to consolidate desert sand in desert areas, forming a hard crust layer on the surface that resists sand suspension and fights sandstorm disasters. (4) The calcite precipitation of EICP is stable and long lasting. Wind tunnel and wetting–drying cycle testing of solidified desert sand showed that it could endure strong winds at maximum wind speeds of 29.1 m/s. Mass loss rates for wetting–drying cycle samples of solidified desert sand at 29.1 m/s were 2.31%, 1.87%, and 0.18% after two, four, and six spraying times, respectively. These tests showed that EICP biomineralization technology clearly diminished the harmful impacts of sandstorms. (5) All tests were completed at environment temperatures of  $10\text{ }^{\circ}\text{C} \pm$ , showing that EICP biomineralization technology has a clear obvious advantage over MICP for solidifying desert sand. EICP is environmentally-friendly and can be applied to reduce sandstorm disaster impacts in arid and semi-arid areas.

## Discussions

Table 3 lists the mass variability for EICP solidified desert sand samples. Increases in mass were due to calcite deposited by EICP consolidation. Calcite deposition solidified the desert sand, forming a hard crust layer on the surface that resisted suspension. Figure 4 contains photos of solidified desert sand samples. It can be seen that the surface color of solidified samples became whiter as spraying time increased. Productive rates of calcite during EICP solidification were measured and calculated in Fig. 5. They were in agreement with the calculated values for calcite during EICP solidification, which decreased as spraying times increased. This was related to the balance between  $\text{CO}_3^{2-}$  and  $\text{Ca}^{2+}$  concentrations and seepage effects of the EICP solution. For these reasons, the surface color of solidified samples appeared more white as spraying time increased in Fig. 4, which indicated that some calcium acetate remained on the surface because the productive rates of calcite did not reach 100%

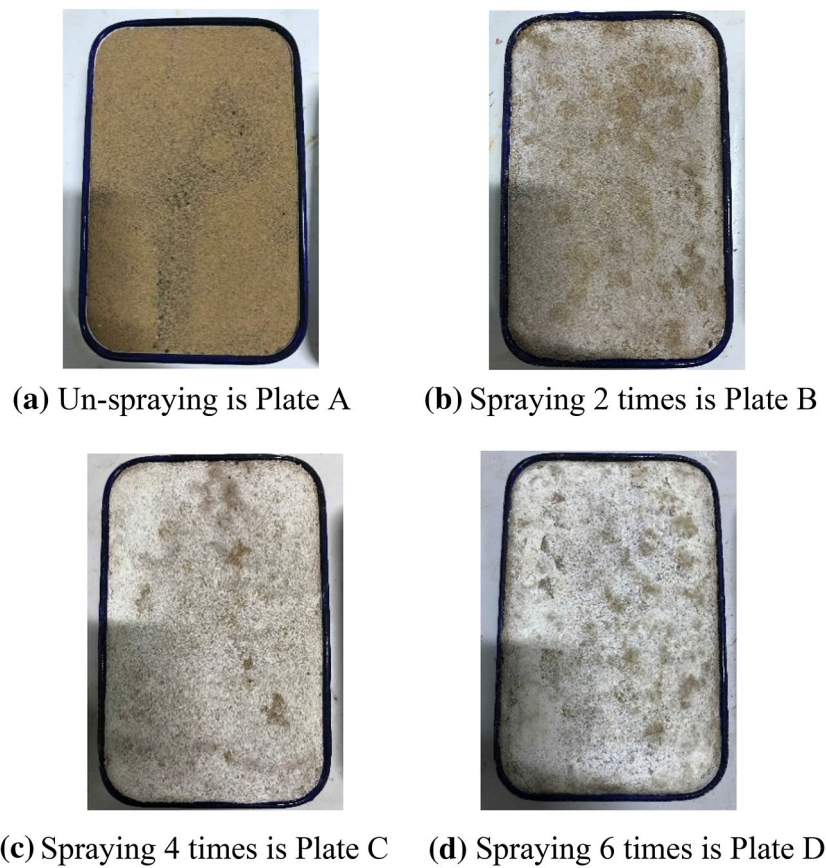


**Figure 4.** Photos of un-solidification and solidification desert sand of EICP.

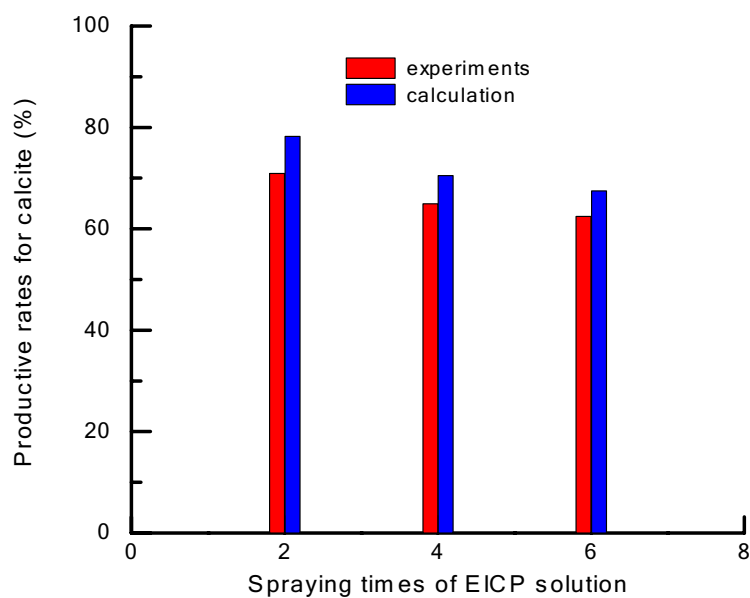


**Figure 5.** Productive rates of calcite during solidification desert sand of EICP.



Spraying times	Initial mass (g)	Wind speed: 14.0 m/s		Wind speed: 22.7 m/s		Wind speed: 29.1 m/s	
		Mass blown (g)	Mass changes (g)	Mass blown (g)	Mass changes (g)	Mass blown (g)	Mass changes (g)
0	2,730	1,736	- 994	1,019	- 1,711	426	- 2,184
2	2,736	2,716	- 20	2,687	- 29	2,626	- 61
4	2,744	2,743	- 1	2,735	- 8	2,691	- 44
6	2,755	2,753	- 1	2,751	- 2	2,749	- 3

**Table 4.** The mass variations of solidified desert sand samples of EICP after blowing at different wind speeds during the wind tunnel tests.

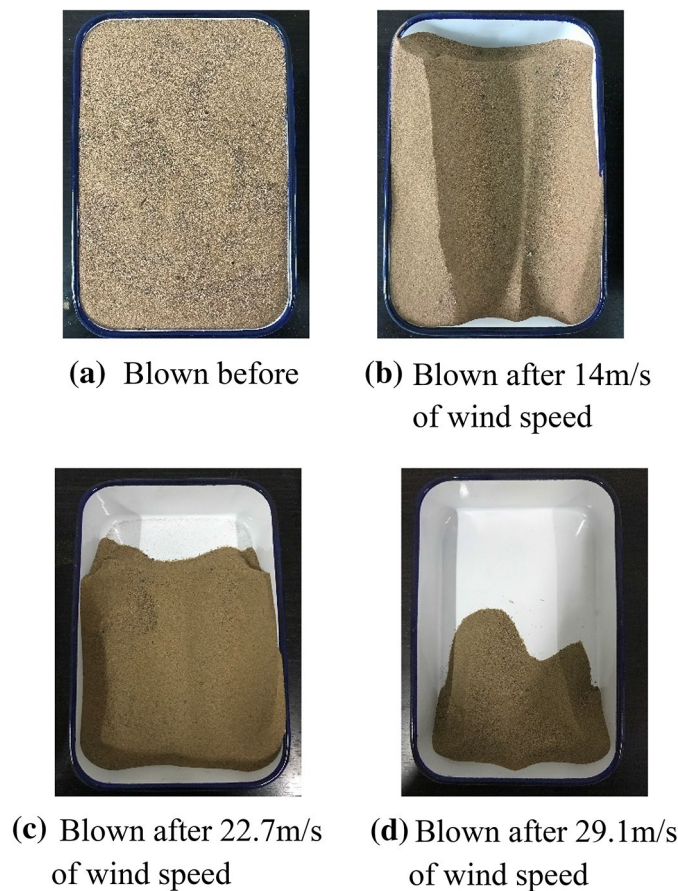


**Figure 6.** Photos of the natural desert sand blown by different strong winds in 1 min.

during EICP solidification. This study attempted to increase the calcite efficiency in the next step to improve the EICP consolidation effects for desert sand.

Table 4 shows the mass variability of natural /solidified desert sand samples after wind tunnel testing. The loss of mass by natural desert sand was large and it was clearly blown upward during wind tunnel tests. The saltation distance and suspension height for natural desert sand were measured when the wind speed reached 7.0 m/s: saltation distance was about 50–60 cm and the suspension height was about 40–45 cm. According to wind tunnel test data in Table 4, the blown mass loss rates for natural desert sand were 36.4%, 62.7%, and 80.0% at wind speeds of 14.0 m/s, 22.7 m/s, and 29.1 m/s, respectively. These tests aided the interpretation of sandstorm disasters because high amounts of desert sand were removed by strong winds in desert areas (Fig. 6).

However, Table 4 shows that the solidified desert sand resisted the strong winds and limited sandstorm impacts. During wind tunnel testing, the solidified desert sand samples did not exhibit the suspension and saltation phenomena of natural desert sand, even if winds were low. Higher EICP spraying times also resulted in better solidification effects of desert sand. According to wind tunnel test results in Table 4, the blown mass loss rates of solidified desert sand were less than 3.0% after two spraying times at wind speeds of 14.0 m/s, 22.7 m/s, and 29.1 m/s. Mass loss rates at a wind speed of 29.1 m/s were 2.23%, 1.61%, and 0.11% after two, four, and six spraying times, respectively. Figures 7, 8, and 9 show photos of solidified desert sand under strong

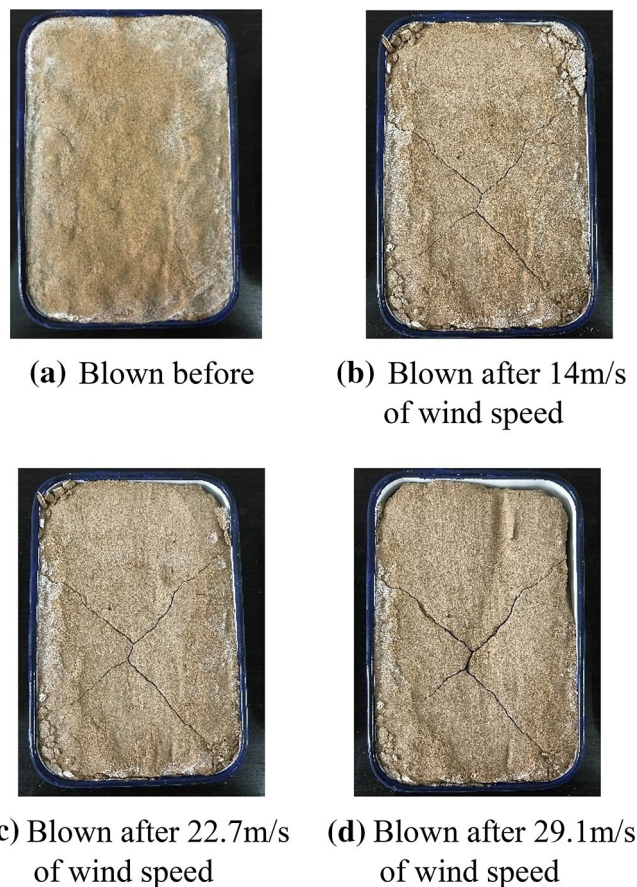


**Figure 7.** Photos of the solidification aeolian sand blown by different strong winds in 1 min. for spraying 2 times of mixture solution of EICP.

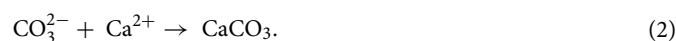
winds at different intensities. They demonstrate that EICP was a good method for solidifying desert sand and can be used to limit sandstorm disaster impacts in desert areas. In addition, EICP tests were completed at low environmental temperatures ( $10\text{ }^{\circ}\text{C} \pm$ ). This means that EICP can acclimate to broader field conditions and may be more widely applied.

Table 5 lists the mass variability of solidified desert sand after wetting–drying cycles at different wind speeds. The lack of mass variability in the samples illustrates that the calcite deposition of EICP was not hydrolyzed and was stable over long time periods. The stability and duration of EICP solidification were also demonstrated by wind tunnel tests on wetting–drying cycle samples. Figure 10 shows that wetting–drying cycle samples resisted the impacts of strong winds and did not experience the same saltation and suspension phenomena at a wind speed of 29.1 m/s. During wind tunnel testing, mass losses were less than 3.0% for wetting–drying cycle samples of solidified sand, and the lost components were partial calcium acetate crystals that remained on the surface. The mass loss rates of wetting–drying cycle samples of solidified desert sand at a wind speed of 29.1 m/s were 2.31%, 1.87%, and 0.18% after two, four, and six spraying times, respectively. Therefore, EICP had long-term application potential for consolidating desert sand and limit sandstorm disaster and combat desertification.

In addition, the cost of consolidating desert sand of EICP is about the same as the grass square method and the cost estimate is based on EICP test effects in the laboratory and field tests<sup>30</sup>.

## Methods

**Characteristics of reactants and urease enzyme.** Urease was extracted from soybeans and purified for use in EICP. It hydrolyses urea ( $\text{CO}(\text{NH}_2)_2$ ) into carbonate ions ( $\text{CO}_3^{2-}$ ) and ammonium ( $\text{NH}_4^+$ ) [Eq. (1)]. The resulting carbonate ions binds with calcium ions ( $\text{Ca}^{2+}$ ) supplied by a calcium acetate solution ( $\text{Ca}(\text{CH}_3\text{COO})_2$ ) to generate calcite precipitate [Eq. (2)].



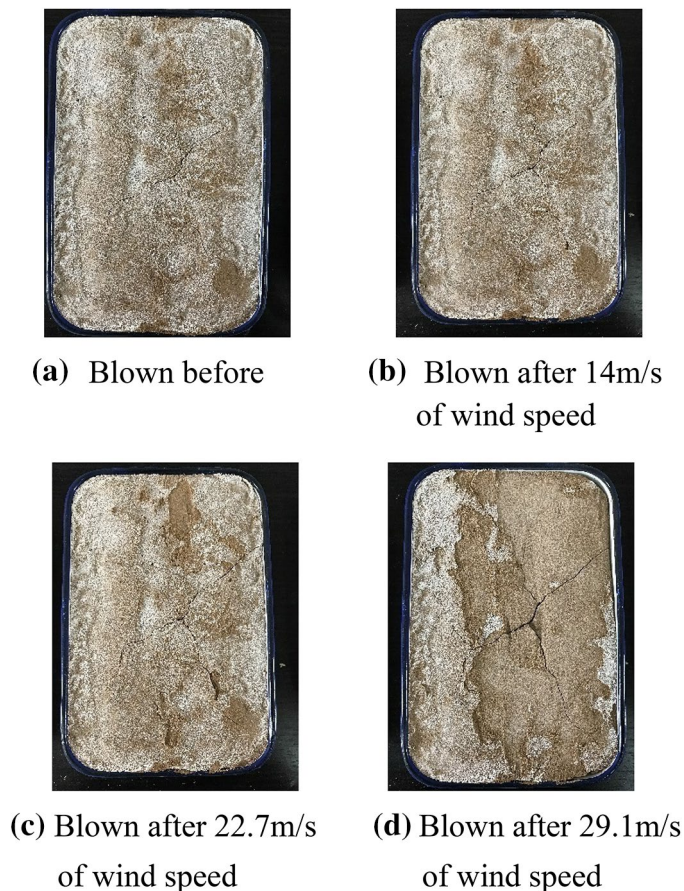


**Figure 8.** Photos of the solidification aeolian sand blown by different strong winds in 1 min. for spraying 4 times of mixture solution of EICP.

**Urea and calcium ion concentrations.** A urea–Ca  $(\text{CH}_3\text{COO})_2$  solution was used for EICP. First, urea was added to a solution of urease with 4,000 U/L (1 U corresponds to the amount of enzyme that hydrolyses 1  $\mu\text{mol}$  of urea per minute at pH 7.0 and 25 °C) and over 48 h the urea was hydrolysed by the urease. Then the urea hydrolysed solution was mixed with calcium acetate solution. The calcium ion concentration in calcium acetate was 0.75 mol/L and the urea concentration was 0.75 mol/L in the EICP solution.

**Water retention feature testing.** Water retention feature tests were conducted by compression with the soil–water retention curve (SWRC) test on unsaturated soils. The sampling density of SWRC was 1.6  $\text{g}/\text{cm}^3$  for natural and solidified desert sand. The size of all samples for water retention feature testing was 61.8 mm in diameter and 20 mm in height. Solidified desert sand samples were sprayed with 10 mL of the EICP mixture solution. Calcium ion and urea concentrations of the EICP solution were 0.75 mol/L as mentioned above. The natural and solidification desert sand samples were saturated prior to water retention tests. During water retention testing, matrix suction was set to increase in 0.5, 1.0, 1.5, 2.5, 5.0, 7.5, 10.0, 15.0, 50.0, 100.0, 150.0 and 200.0 kPa increments for 24 h and tests were only conducted for drying path.

**Temperatures and pH values.** The temperature was  $10\text{ }^\circ\text{C} \pm$  during the EICP reaction and the pH of the solution was 7. Based on the desired engineering application of the enzyme-catalysed mineralization method, the low temperature was controlled during solidification desert sand tests.

**Solidified desert sand.** Four plates were prepared to fill desert sand (A, B, C, and D). Plate size was  $16 \times 24 \times 4$  cm and each plate contained 2,730.0 g of desert sand from Tengger Desert. The EICP solution was sprayed for various durations onto the desert sand on the plate to solidify it. The urea–Ca  $(\text{CH}_3\text{COO})_2$  and urease solutions were sprayed in 50 mL amounts each time for a total amount of 100 mL. Plate A was not sprayed with EICP. Plate B was sprayed twice with 48 h in between. Plate C was sprayed four times in 48 h intervals. Plate D was sprayed six times in 48 h intervals.

**Wind tunnel testing for solidified desert sand.** To evaluate the solidification effects, wind tunnel and drying–wetting cycle testing was conducted on solidified desert sand. The following procedure for wind testing was followed:



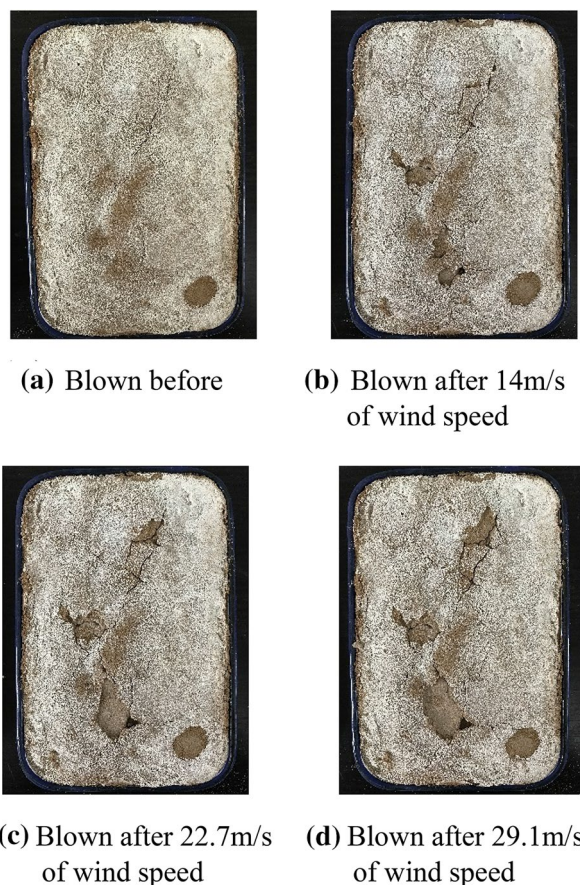


**Figure 9.** Photos of the solidification aeolian sand blown by different strong winds in 1 min. for spraying 6 times of mixture solution of EICP.

Spraying times	Initial mass (g)	Wind speed: 14.0 m/s		Wind speed: 22.7 m/s		Wind speed: 29.1 m/s	
		Mass (g)	Mass changes (g)	Mass (g)	Mass changes (g)	Mass (g)	Mass changes (g)
2	2,736	2,715	- 21	2,684	- 31	2,621	- 63
4	2,745	2,744	- 1	2,738	- 6	2,687	- 51
6	2,756	2,756	0	2,755	- 1	2,750	- 5

**Table 5.** The mass variations of solidified desert sand samples of EICP after blowing at different wind speeds during the wind tunnel tests of wetting–drying cycles.

1. Drying phase: The wet solidified samples of desert sand on plates B, C, and D were kiln-dried in an oven for 8 h at 60 °C in the laboratory and then weighed.
2. Wind tunnel testing: Tests were conducted at three different wind speeds, 14.0 m/s, 22.7 m/s, and 29.1 m/s. Plate A contained natural desert sand, and plates B, C, and D contained solidified desert sand sprayed two, four, and six times with EICP solution, respectively. All plates were placed in a wind tunnel and blown for 1 min at different wind speeds: 14.0 m/s, 22.7 m/s and 29.1 m/s. Then the desert sand samples were weighed again.

**Wetting–drying cycle testing for solidified desert sand.** The following procedure was used for drying–wetting testing:

1. Wetting phase: The solidified samples of desert sand on plates B, C, and D were weighed and then sprayed with 200 mL of tap water, then retained for 24 h in the laboratory.
2. Drying phase: The wet solidified samples of desert sand on plates B, C, and D were kiln-dried in an oven for 8 h at 60 °C in the laboratory, and then weighed. The dried samples of desert sand on plates B, C, and D were stored in the laboratory for a second day.

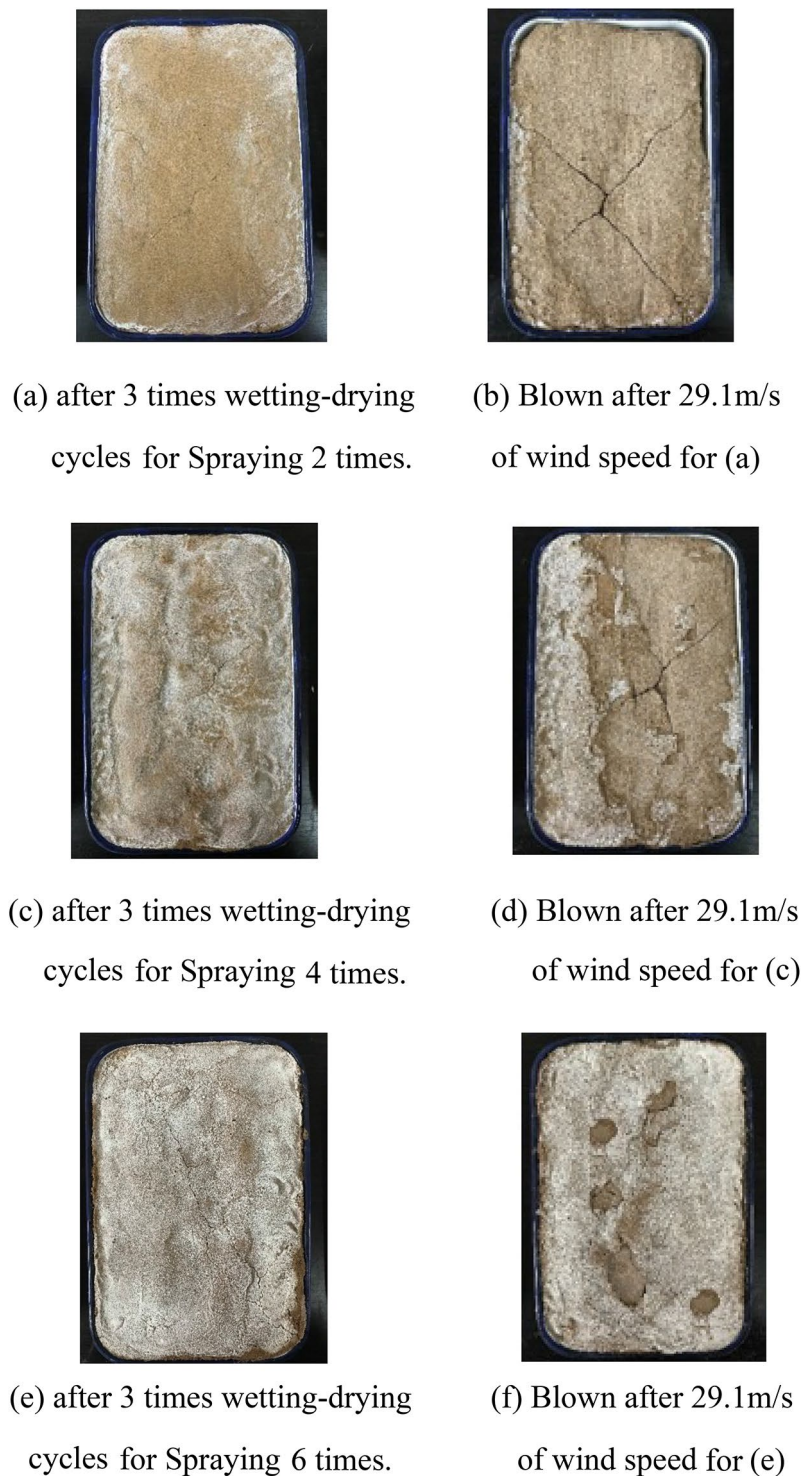


**Figure 10.** Photos of the solidification aeolian sand blown by strong winds in 1 min. after 3 wetting–drying cycles for different spraying times of mixture solution of EICP.

3. The above procedure was repeated for three wetting–drying cycles.
4. Wind tunnel testing: The dried solidified samples of desert sand on plates B, C and D were placed in a wind tunnel and blown for 1 min at different wind speeds, 14.0 m/s, 22.7 m/s and 29.1 m/s. Plates B, C, and D of solidified desert sand samples were weighed after each test.

Received: 28 December 2019; Accepted: 8 June 2020

Published online: 30 June 2020

## References

- Middleton, N. & Thomas, D. S. G. *World Atlas of Desertification* 182 (Arnold, London, 1997).
- Wang, T., Xue, X., Zhou, L. H. & Guo, J. Combating aeolian desertification in northern China. *Land Degrad. Dev.* **26**, 118–132 (2015).
- Le Houérou, H. N. Biogeography of the arid steppeland north of the Sahara. *J. Arid Environ.* **48**, 103–128 (2001).
- Mekuria, W. *et al.* Effectiveness of enclosures to restore degraded soils as a result of overgrazing in Tigray, Ethiopia. *J. Arid Environ.* **69**, 270–284 (2007).
- Wang, F., Pan, X., Wang, D., Shen, C. & Lu, Q. Combating desertification in China: past, present and future. *Land Use Policy* **31**, 311–313 (2013).
- Eslamian, S. & Eslamian, F. A. (eds) *Handbook of Drought and Water Scarcity: Environmental Impacts and Analysis of Drought and Water Scarcity* (CRC Press, Boca Raton, 2017).
- Yang, Y. L., Squires, V., & Lu, Q. *Global Alarm: Dust Storms and Sandstorms from the World's Dry Lands* 346 (UN Publication, 2002).
- McKendry, I. G. *et al.* Long-range transport of Asian dust to the Lower Fraser Valley, British Columbia, Canada. *J. Geophys. Res.* **106**(D16), 18361–18370 (2001).
- Uno, I. *et al.* Asian dust transported one full circuit around the globe. *Nat. Geosci.* **2**(8), 557–560 (2009).
- Grainger, A. *The Threatening Desert: Controlling Desertification* (Routledge, London, 2013).
- Deléglise, C., Loucougaray, G. & Alard, D. Effects of grazing exclusion on the spatial variability of subalpine plant communities: a multiscale approach. *Basic Appl. Ecol.* **12**, 609–619 (2011).
- Liu, J. H., Wu, J. J., Su, H. B., Gao, Z. & Wu, Z. Effects of grazing exclusion in Xilin Gol grassland differ between regions. *Ecol. Eng.* **99**, 271–281 (2017).
- Verdoodt, A., Mureithi, S. M., Ye, L. & Van, R. E. Chronosequence analysis of two enclosure management strategies in degraded rangeland of semi-arid Kenya. *Agric. Ecosyst. Environ.* **129**, 332–339 (2009).
- Witt, G. B., Noël, M. V., Bird, M. I., Beeton, R. J. S. & Menzies, N. W. Carbon sequestration and biodiversity restoration potential of semi-arid mulga lands of Australia interpreted from long-term grazing enclosures. *Agric. Ecosyst. Environ.* **141**, 108–118 (2011).
- Sasaki, T. *et al.* Rainfall variability may modify the effects of long-term enclosure on vegetation in Mandalgobi, Mongolia. *J. Arid Environ.* **73**, 949–954 (2009).
- Slimani, H., Aidoud, A. & Rozé, F. 30 Years of protection and monitoring of a steppic rangeland undergoing desertification. *J. Arid Environ.* **74**, 685–691 (2010).
- Xu, B., Zhang, J., Huang, N., Gong, K. & Liu, Y. Characteristics of turbulent aeolian sand movement over straw checkerboard barriers and formation mechanisms of their internal erosion form. *J. Geophys. Res. Atmos.* **123**(13), 6907–6919 (2018).
- Chou, C. W., Seagren, E. A., Aydilek, A. H. & Lai, M. Biocalcification of sand through ureolysis. *J. Geotech. Geoenviron. Eng.* **137**(12), 1179–1189 (2011).
- Dejong, J. T., Mortensen, B. M., Martinez, B. C. & Nelson, D. C. Bio-mediated soil improvement. *Ecol. Eng.* **36**(2), 197–210 (2010).
- Muynck, W. D., Belie, N. D. & Verstraete, W. Microbial carbonate precipitation in construction materials: a review. *Ecol. Eng.* **36**(2), 118–136 (2010).
- Cuthbert, M. O. *et al.* A field and modeling study of fractured rock permeability reduction using microbially induced calcite precipitation. *Environ. Sci. Technol.* **47**(23), 13637–13643 (2013).
- Montoya, B., DeJong, J. & Boulanger, R. Dynamic response of liquefiable sand improved by microbial-induced calcite precipitation. *Géotechnique* **63**(4), 302–312 (2013).
- Soon, N. W., Lee, L. M., Khun, T. C. & Ling, H. S. Factors affecting improvement in engineering properties of residual soil through microbial-induced calcite precipitation. *J. Geotech. Geoenviron. Eng.* **140**(5), 04014006 (2014).
- Sun, X., Miao, L., Tong, T. & Wang, C. Study of the effect of temperature on microbially induced carbonate precipitation. *Acta Geotech.* **14**(3), 627–638 (2019).
- DeJong, J. T., Fritzsche, M. B. & Nusslein, K. Microbially induced cementation to control sand response to undrained shear. *J. Geotech. Geoenviron. Eng.* **132**(11), 1381–1392 (2006).
- Sun, X., Miao, L., Tong, T. & Wang, C. Improvement of microbial-induced calcium carbonate precipitation technology for sand solidification. *J. Mater. Civ. Eng.* **30**(11), 04018301 (2018).
- Soon, N. W., Lee, L. M., Khun, T. C. & Ling, H. S. Improvements in engineering properties of soils through microbial-induced calcite precipitation. *KSCE J. Civ. Eng.* **17**(4), 718–728 (2013).
- Wijngaarden, W., Vermolen, F., Meurs, G. & Vuik, C. Modelling biogROUT: a new ground improvement method based on microbial-induced carbonate precipitation. *Transp. Porous Media* **87**(2), 397–420 (2011).
- Wu, Y. *et al.* Geophysical monitoring and reactive transport modeling of ureolytically-driven calcium carbonate precipitation. *Geochem. Trans.* **12**(1), 7 (2011).
- Miao, L. C., Wu, L. Y., Sun, X. H., Li, X. & Zhang, J. Z. Method for solidifying desert sands with enzyme-catalysed mineralization. *Land Degrad. Dev.* <https://doi.org/10.1002/ldr.3499> (2019).
- Neupane, D., Yasuhara, H., Kinoshita, N. & Unno, T. Applicability of enzymatic calcium carbonate precipitation as a soil-strengthening technique. *J. Geotech. Geoenviron. Eng.* **139**(12), 2201–2211 (2013).
- Neupane, D., Yasuhara, H., Kinoshita, N. & Unno, T. Distribution of mineralized carbonate and its quantification method in enzyme mediated calcite precipitation technique. *Soils Found.* **55**(2), 447–457 (2015).
- Hamdan, N. K. & Kavazanjian, E. Jr. Enzyme-induced carbonate mineral precipitation for fugitive dust control. *Géotechnique* **66**(7), 546–555 (2016).
- Dakhane, A. *et al.* Crack healing in cementitious mortars using enzyme-induced carbonate precipitation: quantification based on fracture response. *J. Mater. Civ. Eng.* **30**(4), 04018035 (2018).

## Acknowledgements

This work was supported by National Key R&D Program of China (No. 2018YFB1600304) and the National Natural Science Foundation of China (No. 51578147).

## Author contributions

L.M. and L.W. conceived and designed research. L.W. and X.S. conducted experiments. L.M. analyzed data and wrote the manuscript. All authors read and approved the manuscript.

## Competing interests

The authors declare no competing interests.

### Additional information

**Correspondence** and requests for materials should be addressed to L.M.

**Reprints and permissions information** is available at [www.nature.com/reprints](http://www.nature.com/reprints).

**Publisher's note** Springer Nature remains neutral with regard to jurisdictional claims in published maps and institutional affiliations.



**Open Access** This article is licensed under a Creative Commons Attribution 4.0 International License, which permits use, sharing, adaptation, distribution and reproduction in any medium or format, as long as you give appropriate credit to the original author(s) and the source, provide a link to the Creative Commons license, and indicate if changes were made. The images or other third party material in this article are included in the article's Creative Commons license, unless indicated otherwise in a credit line to the material. If material is not included in the article's Creative Commons license and your intended use is not permitted by statutory regulation or exceeds the permitted use, you will need to obtain permission directly from the copyright holder. To view a copy of this license, visit <http://creativecommons.org/licenses/by/4.0/>.

© The Author(s) 2020